Biol. Cybern. 84, 91–101 (2001)

Biological Cybernetics

Dynamics of two electrically coupled chaotic neurons: Experimental observations and model analysis

P. Varona[1,2], **J. J. Torres**[1], **H. D. I. Abarbanel**[1,3], **M. I. Rabinovich**[1], **R. C. Elson**[1]

[1] Institute for Nonlinear Science, University of California, San Diego, 9500 Gilman Dr., La Jolla, CA 92093-0402, USA
[2] GNB. Dpto. de Ingeniería Informática, ETSI. UAM, 28049 Madrid, Spain
[3] Department of Physics and Marine Physical Laboratory, Scripps Institution of Oceanography, University of California, San Diego, USA

Received: 28 June 1999 / Accepted in revised form: 30 June 2000

Abstract. Conductance-based models of neurons from the lobster stomatogastric ganglion (STG) have been developed to understand the observed chaotic behavior of individual STG neurons. These models identify an additional slow dynamical process – calcium exchange and storage in the endoplasmic reticulum – as a biologically plausible source for the observed chaos in the oscillations of these cells. In this paper we test these ideas further by exploring the dynamical behavior when two model neurons are coupled by electrical or gap junction connections. We compare in detail the model results to the laboratory measurements of electrically-coupled neurons that we reported earlier. The experiments on the biological neurons varied the strength of the effective coupling by applying a parallel, artificial synapse, which changed both the magnitude and polarity of the conductance between the neurons. We observed a sequence of bifurcations that took the neurons from strongly synchronized in-phase behavior, through uncorrelated chaotic oscillations to strongly synchronized – and now regular – out-of-phase behavior. The model calculations reproduce these observations quantitatively, indicating that slow subcellular processes could account for the mechanisms involved in the synchronization and regularization of the otherwise individual chaotic activities.

1 Introduction

In a series of experiments reported in Elson et al. (1998), we measured and analyzed the synchronization between two pyloric dilator (PD) neurons from the stomatogastric ganglion (STG) of the California spiny lobster *Panulirus interruptus*. These two neurons are coupled by an electrical or gap junction coupling. With the natural magnitude and polarity of the coupling conductance (of approximately 200 nS) one observes synchronization between the slow bursting oscillations of the neurons, but the faster spiking oscillations are not synchronized.

In those experiments we added parallel, artificial electrical coupling between the two neurons by a dynamic current-clamp device (Sharp et al. 1992), allowing us to alter both the magnitude and the polarity of the effective coupling conductance. When the conductance was strengthened, the neurons were observed to fire in strong synchronization, with both bursts and spikes now synchronized. When the effective conductance – natural plus artificial – was lowered to nearly zero, each neuron fired in an irregular, chaotic pattern, and the two neurons were not correlated in their oscillations. When the effective conductance was set to negative values around -75 nS, the two PD neurons were observed to burst in synchrony again, but now out-of-phase. The neuronal activity was regular and periodic in this situation.

Earlier experiments in our laboratory established that the oscillations of isolated PD (and other) neurons from the pyloric central pattern generator (CPG) of the STG are chaotic (Abarbanel et al. 1996). We have previously built a conductance-based model (Falcke et al. 2000) of an STG neuron with realistic biological mechanisms that lead to chaotic oscillations. We have shown that this class of model neuron generates membrane voltage time series whose underlying nonlinear dynamics appears very similar to those of the biological neurons on the pyloric CPG (Falcke et al. 2000), in particular, that of the lateral pyloric (LP) neuron. Here we analyze the synchronization of two such model neurons while they are electrically coupled with varying conductances. The neurons in our experiments were PD neurons from the pyloric CPG, and here we report an extension of our earlier modeling effort that provides an independent test of the properties of the model in a series of settings that were not considered when the model was originally developed.

An essential feature of the neuron model is the slow calcium dynamics that includes the exchange of calcium between the cytoplasm and an intracellular store. A

Correspondence to: P. Varona
(e-mail: pvarona@lyapunov.ucsd.edu)

familiar set of membrane ionic currents underlies the spiking-bursting activity of the neurons. There is at present no direct evidence for this calcium dynamics in measurements on STG neurons, although similar mechanisms occur in other neurons. In that light we must regard the model as biologically plausible rather than biologically verified. The calculations reported here add substantial strength to the plausibility of the model itself, as well as providing a possible explanatory framework for the experiments.

In this paper we demonstrate that the calcium dynamics and ionic currents model describes the sequence of synchronization experiments with PD cells from the lobster's STG reported in Elson et al. (1998). Here, the experimental setup is represented by two model neurons interacting via a simple electrical connection ($I_{ec} = g_{ec}(V_1(t) - V_2(t))$) involving the membrane voltages in the soma-neuropil compartment of neuron one $V_1(t)$ and of neuron two $V_2(t)$. Each model neuron has two compartments, one for the soma-neuropil activity and one for the axon. This circuitry is shown in Fig. 1 which also includes a diagram of the model arrangement in the experiments.

In this paper we first review the model that we have constructed for individual neurons, and discuss aspects of the experiments that we propose to explain with our modeling. Then we discuss the coupling of the two neurons and compare the results of the computations with the experimental data. We point out the role of the slow subcellular dynamics in the behavior of the two coupled neurons. Finally we provide a discussion of the biological importance of the results as well as showing their relevance to nonlinear dynamics as an interesting system with synchronization of chaotic oscillators.

2 The model for individual neurons

For the simulations described in this paper we used a modified version of the single neuron model developed in Falcke et al. (2000). This model neuron has two compartments. One compartment describes three fast currents in the axon region. These are:

1. A fast Na^+ current I_{Na}: this current generates spikes when the axon compartment membrane voltage $V_a(t)$ is above firing threshold.
2. A delayed-rectifier K^+ current I_K which repolarizes the membrane during spike generation.
3. An axonal leak current I_{La}.

In the soma-neuropil compartment we have five membrane currents. These are:

1. A small maximum conductance Ca^{2+} current I_{Ca1}. This current has a fast, low-voltage activation. It inactivates on a slower time scale. The major function of I_{Ca1} is to initiate the transition from low membrane voltage to the plateau level.
2. A large maximum conductance Ca^{2+} current I_{Ca2}. This current sustains the plateau. It activates at a higher voltage than I_{Ca1} and does not inactivate.
3. A hyperpolarization-activated inward current I_h. This current is responsible for restorative depolarization following a strong hyperpolarization of the membrane.
4. A Ca^{2+}-dependent K^+ current $I_{K(Ca)}$. This current activates at high voltage. It increases with cytosolic $[Ca^{2+}]$. It is crucial for the termination of the plateau.
5. A somatic leak current I_L.

In addition, the soma-neuropil compartment contains Ca^{2+} dynamics that describe uptake and release by the

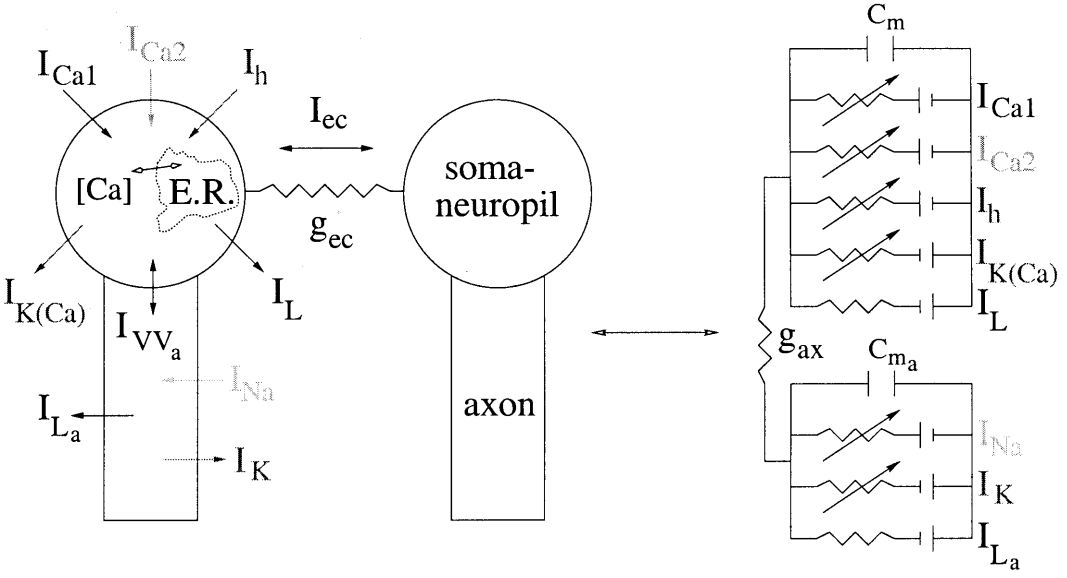

Fig. 1. Model of two pyloric dilator (PD) neurons from the pyloric central pattern generator (CPG) coupled electrically by a coupling $I_{ec} = g_{ec}(V_1(t) - V_2(t))$, where $V_1(t)$ and $V_2(t)$ are the membrane voltages in the soma of neuron one and neuron two, respectively. The model includes a detailed description of the Ca^{2+} storage and transport in the endoplasmic reticulum (ER) of each neuron (Falcke et al. 2000) whose dynamics is slower than the average bursting period

endoplasmic reticulum (ER) to the cytosol, regulated by an intracellular messenger: inositol 1,4,5-triphosphate (IP_3). The calcium concentration dynamics in the ER is slower (by about three times in this model) than the characteristic time constant of the membrane potential oscillations. We have, at present, no direct evidence for this pathway for calcium control in STG neurons, but it has been already observed in many types of neurons and excitable cells (Otsu et al. 1990; Satoh et al. 1990; Walton 1991; Sharp et al. 1993; Martone et al. 1997). Varying the concentration of IP_3 allows the model neuron to produce both regular oscillations and chaotic behavior. In our investigation of this model we made a quantitative nonlinear comparison between the model output and observed data from an LP neuron in the pyloric CPG of the STG. This nonlinear analysis of the model and of the experimental time series reveals that each produces low-dimensional dynamics with three or four active degrees of freedom. The model has twelve independent dynamical variables, and these contract to a subspace of the full state space of the system. The living neuron has at least this number of ion channels and certainly numerous other dynamical degrees of freedom. It too exhibits low-dimensional dynamical behavior, which we demonstrate in the examples discussed below.

While we built this model with data from an LP neuron in mind, we have found it also applies to the other individual neurons in the pyloric CPG that we have observed in the laboratory. In particular, it yields a very good description of the isolated PD neuron. This is achieved in the model by small alterations in the kinetics (a -15 mV shift) and maximal conductances for some of the ion channels ($g_{Na} = 77\,\mu S$, $g_{Ca1} = 0.162\,\mu S$ – cf. Falcke et al. (2000) p. 526). The calculations shown in this paper correspond to this PD version of the model.

In Fig. 2 we show the phase portraits from the soma-neuropil voltage time traces from the PD model output, and from the measured soma membrane voltage from an isolated PD neuron observed in the experiments. Each phase portrait is constructed by using the voltage $V(t)$ and two time lags to make three-dimensional vectors $[V(t), V(t+T), V(t+2T)]$ where the time lag T is chosen using average mutual information as described in Abarbanel (1996) and Falcke et al. (2000). We have also evaluated the other nonlinear statistical quantities characterizing the chaotic oscillations of the individual experimental and model PD neurons. These also agree, but we do not reproduce those results here as they are analogous to those reported in Falcke et al. (2000) for the LP neuron.

A complete description of the currents, in terms of the conductance variables described by Hodgkin-Huxley and Goldman-Hodgkin-Katz formalisms and of the calcium dynamics, can be found in Falcke et al. (2000). Note the changes mentioned above to adapt the model to the behavior of the PD neurons. For the simulations described in this paper, $[IP_3]$ was set at 0.356 μM. With this value each model neuron fires with chaotic spiking-bursting activity similar to that of the isolated PD cells. Time courses from the experimental observations and from the model are shown in Fig. 3. The experimental time series illustrated and analyzed in this paper come from the same, or very similar, experiments as those described in Elson et al. (1998). The experimental methods and protocols are summarized in that paper.

3 Results of model simulations

In the physiological experiments we studied the oscillations of the coupled PD neurons over a broad range of additional external couplings g_a (Elson et al. 1998). In the models the net coupling between the neurons is denoted g_{ec}. Its relation to the total coupling reported in Elson et al. (1998) is approximately $g_{ec} \approx g_a$ + (50–200) nS, the last term corresponding to the natural coupling between the cells. In varying g_a we showed that the oscillations undergo a bifurcation from strongly synchronized behavior when $g_a > 0$, namely adding to the natural dissipative coupling, through essentially decoupled chaotic oscillations of the PD neurons when $g_a \approx -200$ nS, and resulting in regularized anti-synchronized or anti-phase oscillations when $g_a \approx -275$ nS. In

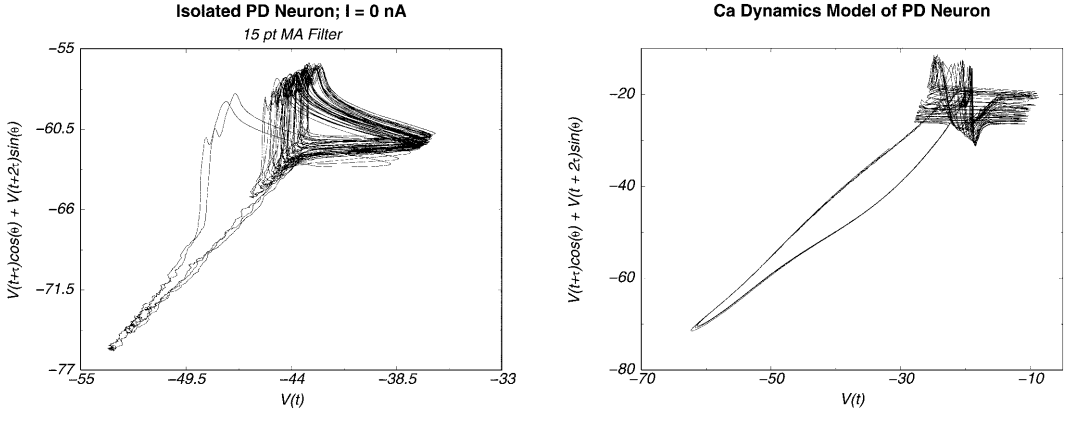

Fig. 2. Comparison of the time-delay phase portraits for the observed isolated PD neuron from the pyloric CPG of lobster, and in our model for the PD neuron as described in the text. The coordinates in each plot are the membrane voltage in the soma region $V(t)$ and its time delays: $V(t), V(t+T)$, and $V(t+2T)$. The time lag T is selected using average mutual information (Abarbanel 1996; Falcke et al. 2000)

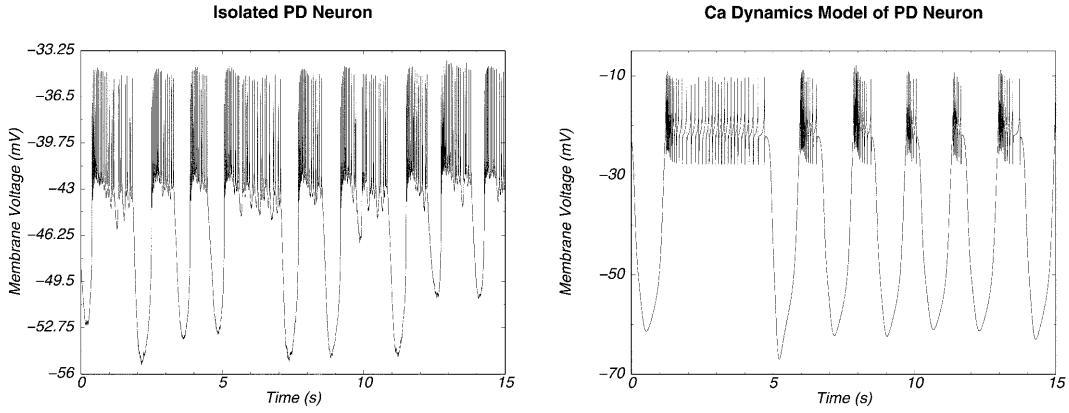

Fig. 3. Time courses for the membrane potential from an observed isolated PD neuron in the pyloric CPG of lobster, and in our model for the PD neuron as described in the text

this paper we report on model results for the coupled PD neurons particularly for four values of g_{ec}:

1. $g_{ec} \approx 0$–0.01 nS, which leads to independent chaotic oscillations of the two neurons. This corresponds to $g_a \approx -200$ nS in the experiments (Elson et al. 1998).
2. $g_{ec} \approx 50$ nS, which leads to burst, but not complete spike, synchronization. This corresponds to $g_a = 0$ nS in the experimental system.
3. $g_{ec} \geq 200$ nS, which leads to total synchronization of burst and spike oscillations, corresponding to $g_a > 0$ nS in the experiments.
4. $g_{ec} \approx -1$ nS, which leads to regular, out-of-phase burst oscillations. In the experiments, this corresponds to $g_a \leq -200$ nS.

Now we discuss the results of the simulations for the membrane voltage for each of the PD neurons, the cytoplasmic concentration of calcium $[Ca^{2+}]$ and the concentration of calcium $[Ca^{2+}]_{ER}$ in the ER, at each of the four settings of g_{ec} just noted. As we will see, the cooperative activity of the neurons shows a strong dependence on the slow $[Ca^{2+}]_{ER}$ dynamics of each cell.

3.1 Independent chaotic behavior

When the two model neurons are coupled with null or small coupling conductance (here $g_{ec} \approx 0.01$ nS), independent chaotic behavior of the two PD neurons is observed in the simulations. For each neuron the widths of the membrane potential bursts range from half a second to two seconds oscillating in a nonperiodic fashion as we show in the top panel of Fig. 4. The number of spikes on the top of the slow waves also

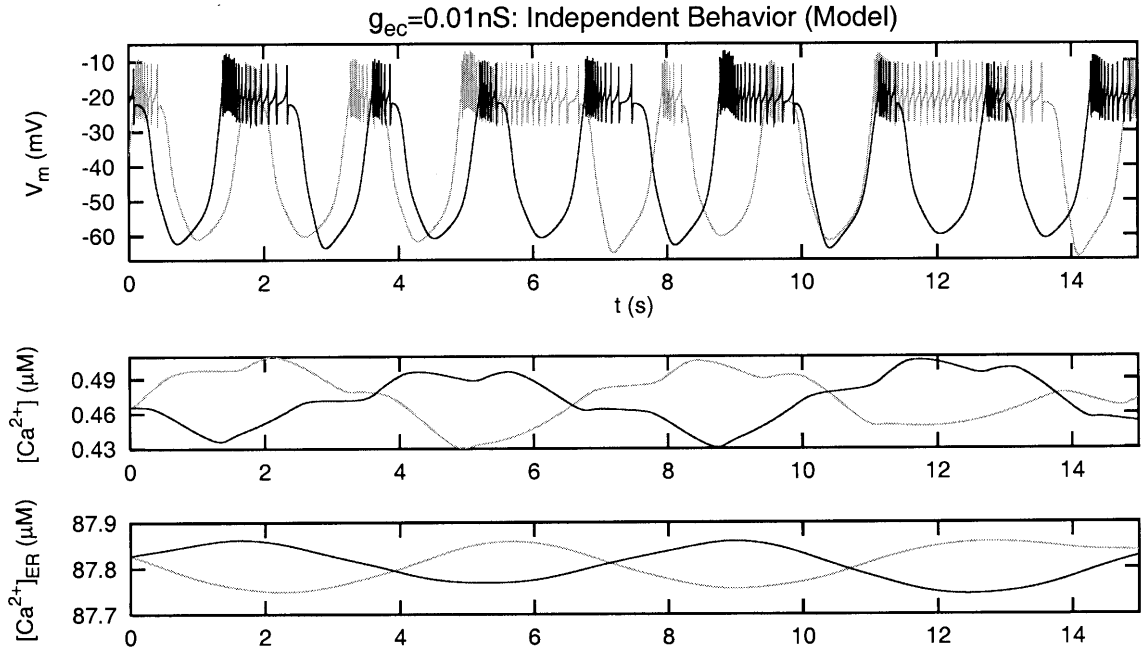

Fig. 4. Independent chaotic bursting activity when the two PD model neurons are connected with a small coupling conductance $g_{ec} = 0.01$ nS. Activity for neuron one is plotted with a *dark trace*, while neuron two is shown as a *light trace*. From *top* to *bottom*: membrane potential, cytoplasmic calcium concentration $[Ca^{2+}]$, and calcium concentration inside the endoplasmic reticulum $[Ca^{2+}]_{ER}$

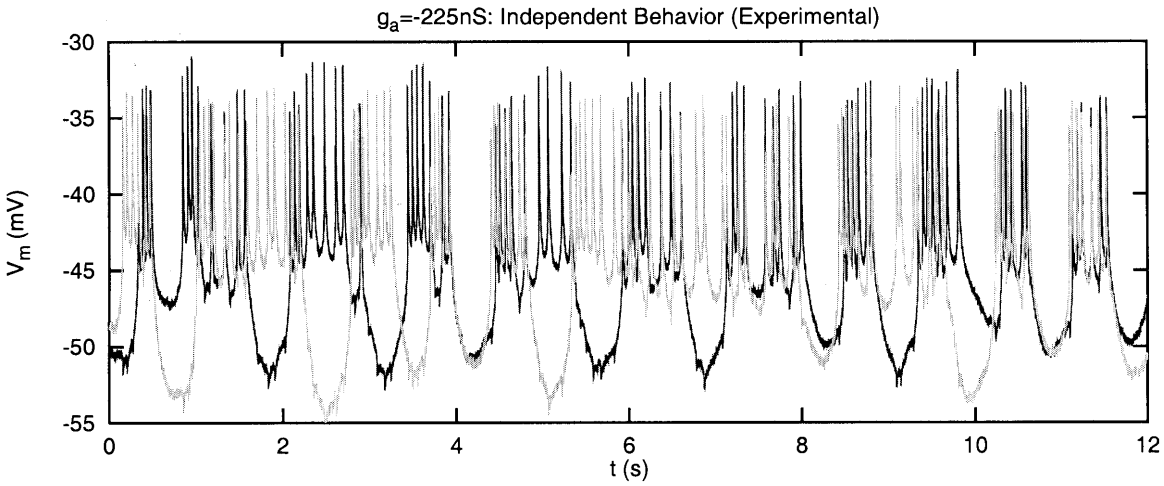

Fig. 5. Observed time courses for two biological PD neurons with effective electrical coupling close to 0 nS. Activity for neuron one is plotted with a *dark trace*, while neuron two is shown as a *light trace*. This data resembles that in Fig. 2b of Elson et al. (1998)

changes from burst to burst. In the middle and lower panels of Fig. 4 we note that local maxima of $[Ca^{2+}]$ mark the end of the burst plateaus, due to the action of $I_{K(Ca)}$. $[Ca^{2+}]_{ER}$ evolves more slowly, modulating the faster oscillations of $[Ca^{2+}]$ in anti-phase. For comparison we also show in Fig. 5 the observed time courses of two PD neurons with their effective coupling near zero; this corresponds to $g_a \approx -200$ nS in Elson et al. (1998).

The chaotic behavior of the individual PD neurons has been checked by evaluating their Lyapunov exponent spectrum. One positive Lyapunov exponent, and a Lyapunov dimension of 4.75 is found for both the observed and the computed time series.

3.2 Partial synchronization

When we set $g_{ec} \approx 50$ nS we see burst synchronization, but spike synchronization is not complete. This is shown in Fig. 6 and also in the plot of $V_1(t)$ vs $V_2(t)$ (shown later in Fig. 13). Note the unsynchronized spikes on top of the slow waves in the 1st, 2nd, 4th, 7th and 8th bursts (dark trace vs light trace).

This synchronization of the slow waves is the observed behavior for two living stomatogastric PD neurons interacting with their natural electrical coupling (Fig. 7). Note that in the simulations for this conductivity range, $[Ca^{2+}]$ and the slower $[Ca^{2+}]_{ER}$ oscillate in a similar fashion for both neurons, but they

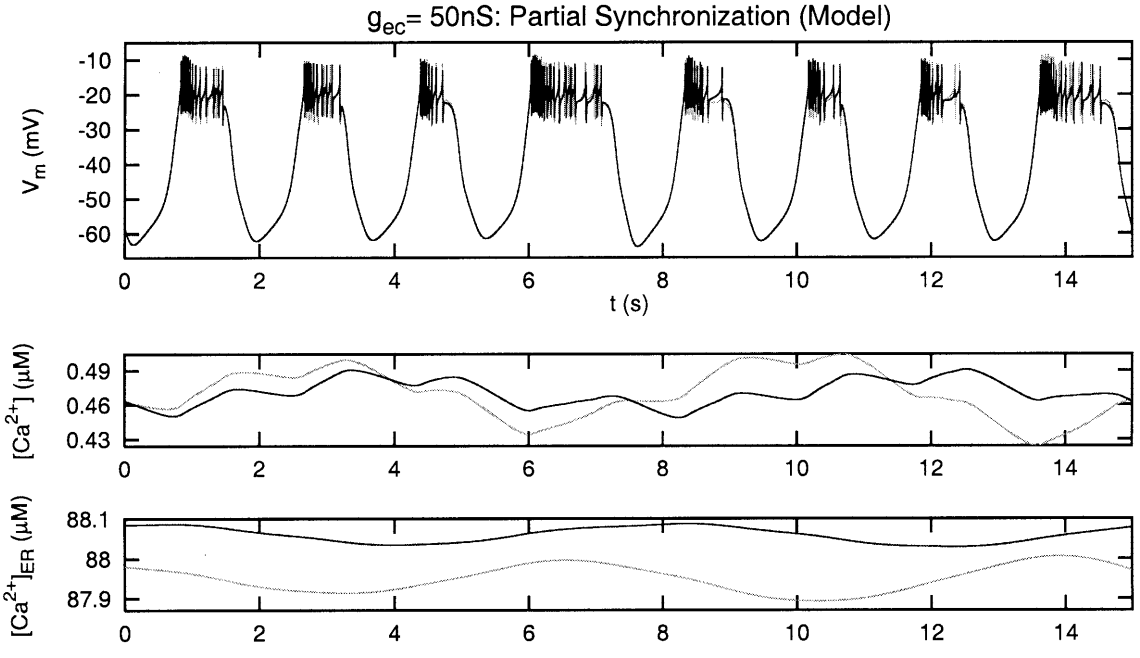

Fig. 6. Burst synchronization when the two PD model neurons are connected with $g_{ec} = 50$ nS. Fast action potentials are not synchronized (see also Fig. 13). This corresponds to the natural state of the PDs in the lobster STG (Elson et al. 1998)

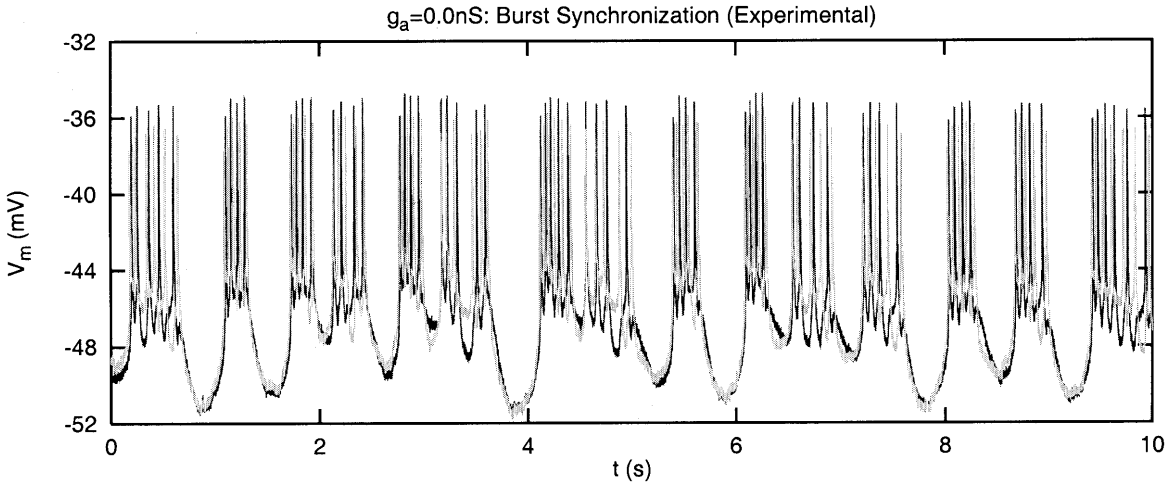

Fig. 7. Observed time courses for two biological PD neurons with effective electrical coupling in its natural state of about 50–200 nS. Activity for neuron one is plotted with a *dark trace*, while neuron two is shown as a *light trace*. This data corresponds to that in Fig. 2a of Elson et al. (1998)

are not completely in-phase between the cells, despite the existing burst synchronization in the membrane potential.

3.3 Total synchronization

Whenever the two model neurons are coupled with a high electrical conductance ($g_{ec} > 200$ nS), complete synchronization both for slow waves and fast action potentials is observed. We show this in Fig. 8 and also in the $V_1(t)$ vs $V_2(t)$ plot for the membrane potentials that we show later in Fig. 13. Here we define complete or total synchronization when the spike time difference between the two neurons is considerably less than the interspike interval in each cell (see Fig. 14 for a quantitative analysis of the synchronization). Again, for this case $[Ca^{2+}]$ and $[Ca^{2+}]_{ER}$ do not oscillate in phase between the two neurons in spite of the overlapping of their membrane potentials.

For all three cases discussed so far (i.e. small, medium and high positive coupling conductance), the bursting activity remains irregular regardless of the degree of synchronization. When burst synchronization does occur, as for $g_{ec} = 200$ nS, we still do not have regular oscillations.

3.4 Anti-phase synchronization and regularization

When the two neurons are coupled with a small negative conductance $g_{ec} = -1$ nS, thus inverting the polarity of

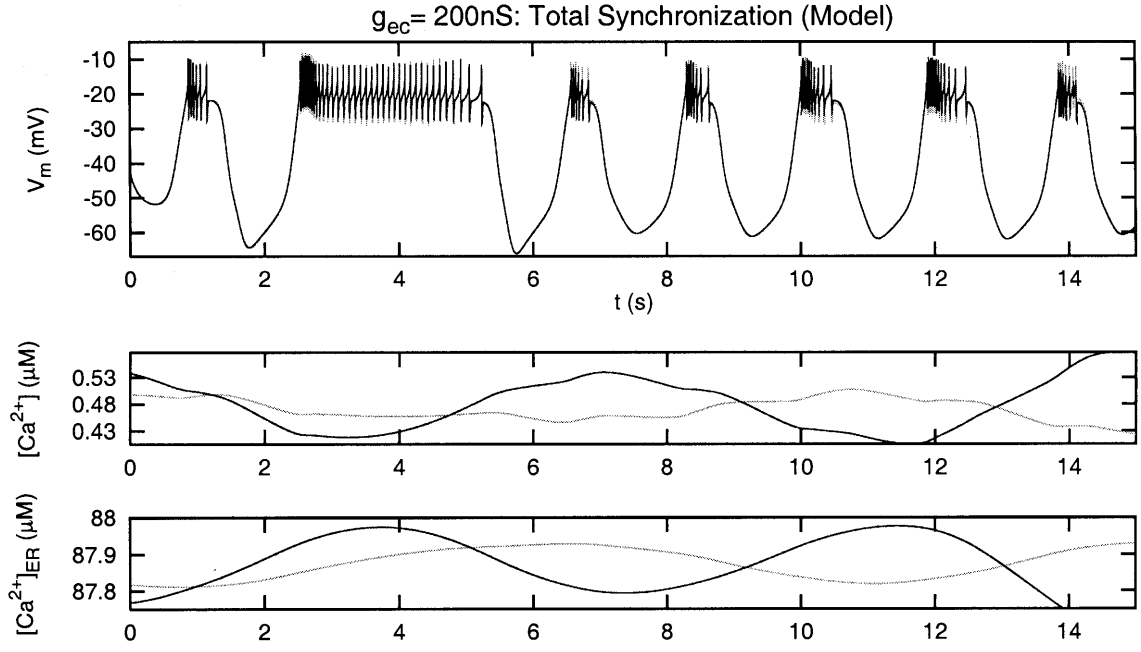

Fig. 8. When the two model PD neurons are connected with a high value for the coupling conductance (here $g_{ec} = 200$ nS), we have complete synchronization of both the slow bursting waves and the faster spiking oscillations (see also Fig. 13)

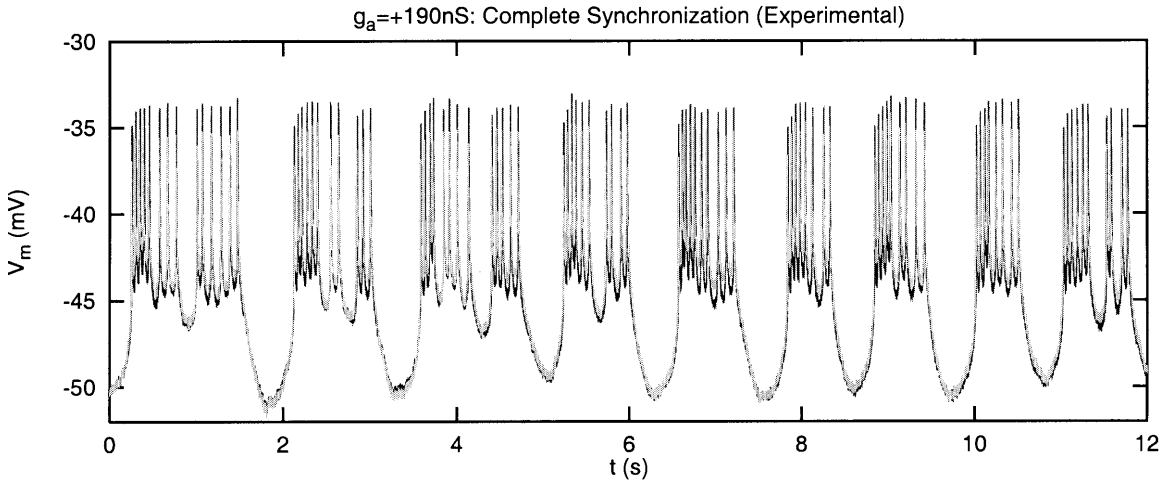

Fig. 9. Observed time courses for two PD neurons with an electrical coupling larger than in their natural state. Activity for neuron one is plotted with a *dark trace*, while neuron two is shown as a *light trace*. Total synchronization of the slow waves and fast spikes is observed

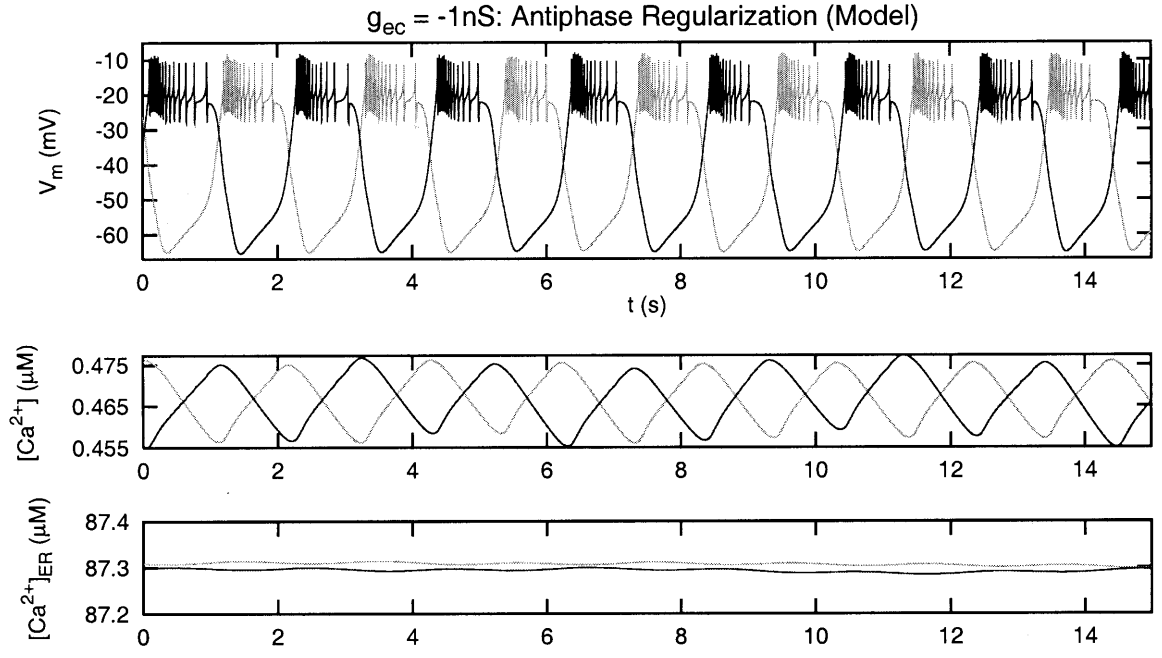

Fig. 10. Regularization in anti-phase behavior when the two model PD neurons are coupled with small negative conductance that inverts the polarity of the current from the electrical coupling $g_{ec} = -1$ nS

the current coming from the electrical coupling in both neurons, anti-phase synchronization is observed in the membrane potentials. We show this behavior in Fig. 10. Furthermore, the two neurons regulate their bursting behavior in the sense that the lengths of the bursts are now uniform. Very similar behavior occurs in the biological neurons, see Fig. 11. As can be seen in the bottom panel of Fig. 10, $[Ca^{2+}]_{ER}$ remains nearly constant for the two neurons, while $[Ca^{2+}]$ oscillates regularly but in anti-phase with respect to the other neuron. In the previous cases $[Ca^{2+}]_{ER}$ oscillated slowly (about three times slower than the average burst period) over a wide amplitude. This can be seen in the bottom panels of Figs. 4, 6, and 8.

For a small negative electrical coupling, $[Ca^{2+}]_{ER}$ in both coupled neurons remains nearly constant since the fast oscillations of calcium in the cytoplasm are rapid and regular enough (in time and amplitude) to have no influence on the slower calcium exchange through the ER membrane. In an individual neuron, allowing $[Ca^{2+}]_{ER}$ to vary leads to chaotic oscillations (Fig. 12, top). However, fixing $[Ca^{2+}]_{ER}$ at a constant value induces periodic bursting and spiking (Fig. 12, bottom). We infer that the steady values of $[Ca^{2+}]_{ER}$ occurring with negative coupling in turn induce regular bursting. Thus, any cooperative behavior that makes the $[Ca^{2+}]_{ER}$ remain nearly constant will result in regular spiking-bursting activity.

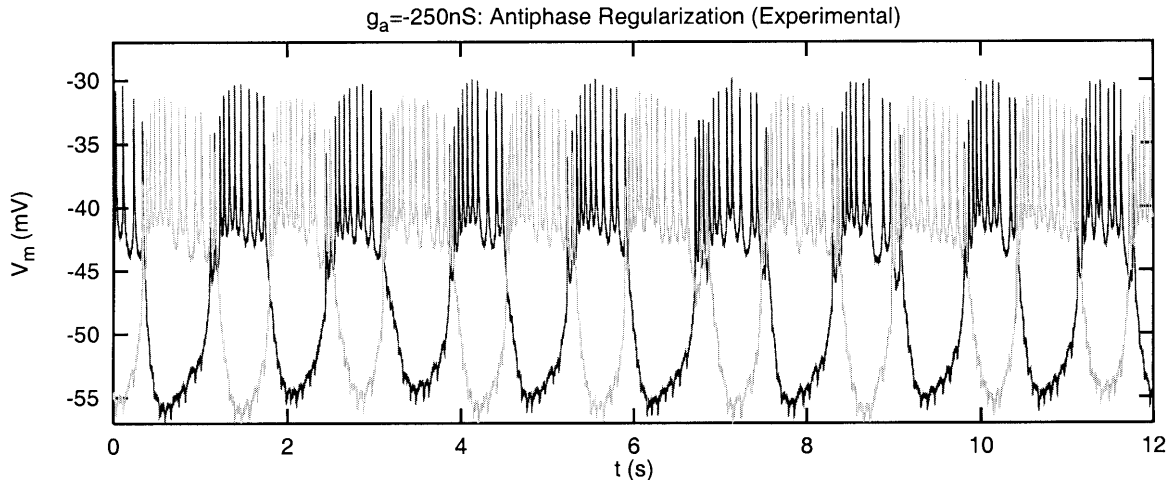

Fig. 11. Observed time courses for two biological PD neurons with negative effective electrical coupling. Activity for neuron one is plotted with a *dark trace*, while neuron two is shown as a *light trace*. This data is similar to that of Fig. 2c of Elson et al. (1998)

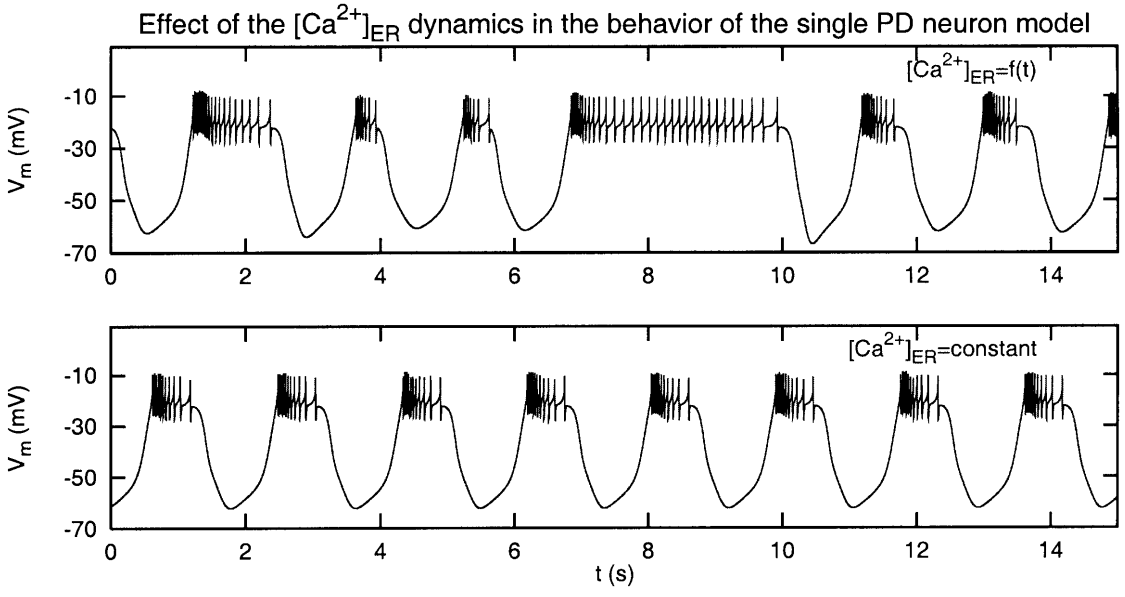

Fig. 12. *Top*: irregular behavior in the isolated neuron when endoplasmic calcium exchange is present in the model; $[Ca^{2+}]_{ER}$ dynamics is determined by the equations in Falcke et al. (2000). *Bottom*: $[Ca^{2+}]_{ER}$ is held fixed, and regular bursting and spiking behavior occurs

3.5 Quantitative analysis

Regarding the synchronization of the activities we summarize the four cases of coupled biological and model PD neurons discussed in this paper in Fig. 13. This figure plots $V_1(t)$ against $V_2(t)$, showing the synchronization status for both slow and fast oscillations depending on the value of the electrical coupling conductance between the two neurons. The coupling conductance is the only parameter changed in the four cases illustrated here: independent chaotic bursting activity, slow wave synchronization, total chaotic synchronization and anti-phase regularized synchronization. Both the biological activity (left panel with dark trace) and model results (right panel with light trace) are shown in this figure. The remarks about the definition of total synchronization in Sect. 3.3 have to be taken into account for the correct interpretation of Fig. 13.

For a more precise quantitative analysis of synchronization of the two model neurons, we adopted a technique developed for the experimental studies of chaos synchronization in electronic circuits. This technique was also used in the analysis of the experimental time series of the two PD cells in Elson et al. (1998). To analyze the synchronization of the slow bursts we suppressed the spikes in the recorded signals using a low-pass filter and studied the slow trajectories given by the filtered signals $V_{F1}(t)$ and $V_{F2}(t)$. To quantify synchronization, we calculated the difference $V_{FD}(t) = V_{F1}(t) - V_{F2}(t)$, and plotted the normalized standard deviation $\sigma_N = \sigma_{V_{FD}}/\sigma_{V_{F1}}$ and normalized maximal deviation $\Delta_N = |V_{FD}|^{max}/(V_{F1}^{max} - V_{F1}^{min})$ as a function

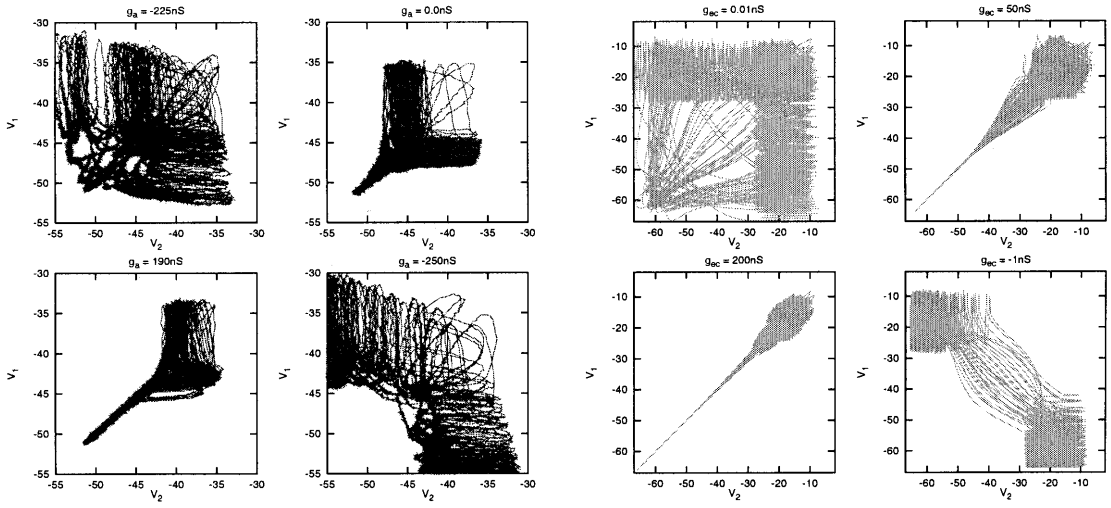

Fig. 13. Membrane potentials V_1 vs V_2 for all four cases discussed in this paper. *Left* (*dark trace*): biological recordings. *Right* (*light trace*): model results. In each panel, from *left* to *right* and *top* to *bottom*: independent bursting activity, slow wave synchronization, total synchronization and anti-phase synchronization ($g_{ec} \approx g_a$ + 50–200 nS)

of g_{ec} (see Fig. 14, left panel). Note the new values of g_{ec} considered in addition to those discussed in the previous sections. The regions of regularized anti-phase behavior, independent activity, and synchronized activity can be easily distinguished in this figure.

We also quantified the synchronization of the fast spike oscillations. Note that the standard criterion for identical synchronization fails here because of small fluctuations in spike timing between the two neurons (much smaller than the characteristic interspike interval in each cell for the case defined as "complete" synchronization). Therefore, we applied a different analysis by measuring the phase relation between spikes. In this analysis we plotted a histogram of the phase, $\Delta\Phi_i$, of the ith spike of neuron 2 within the interval formed by the neighboring pair of spikes in neuron 1 (designated jth and kth, respectively), using the function: $\Delta\Phi_i = 180^\circ(t_i^{(2)} - t_j^{(1)})/|t_j^{(1)} - t_k^{(1)}|$. Here $t_i^{(2)}$ represents the time of spike peak i for neuron 2. The results of this analysis for the time series corresponding to chaotic total ($g_{ec} = 200$ nS) and partial ($g_{ec} = 50$ nS) synchronization are shown in the right panels of Fig. 14. This figure allows us to draw a clear distinction between complete (spike) and partial (burst) synchronization for the analyzed time series.

4 Conclusions and discussion

In the pyloric CPG of the lobster stomatogastric ganglion we find two PD cells connected with gap junction couplings with a conductance value such that

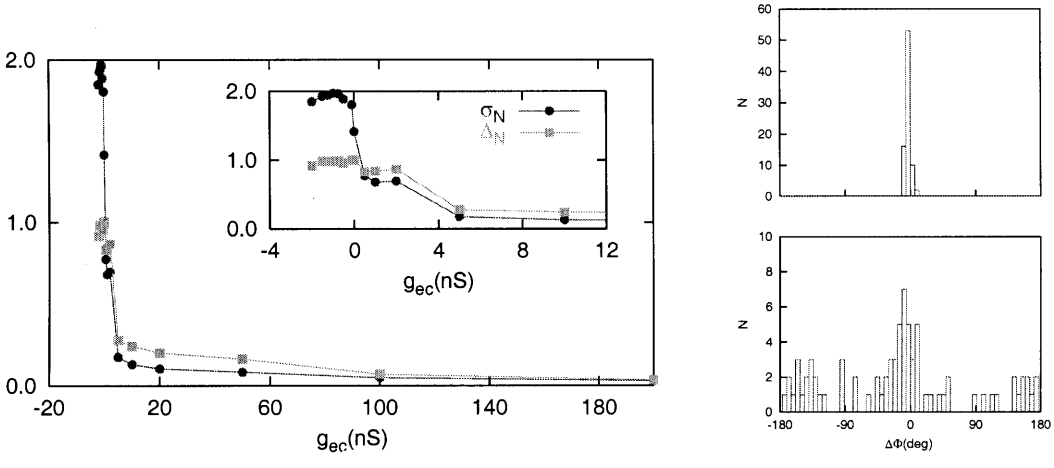

Fig. 14. *Left*: normalized standard deviation σ_N and normalized maximal deviation Δ_N in the slow waves, as defined in the text, as a function of the conductivity through the electrical synapse g_{ec}. The inset shows a blowout of the region where the bifurcations among anti-phase regularized activity, independent behavior and partial chaotic synchronization occur. *Right*: analysis of the synchrony in the fast spiking activity showing the distributions of the phase lags between the spikes in the cases of total ($g_{ec} = 200$ nS, *top*) and partial ($g_{ec} = 50$ nS, *bottom*) synchronization

they produce synchronized oscillations of the slow burst waves of these neurons. The spiking oscillations which ride on top of the bursting activity are not synchronized in the natural state of the coupled PD neurons (Elson et al. 1998). We have reported experiments on these coupled PD neurons which show that as we externally vary the strength of the electrical coupling between them, we can alter the state of the synchronized oscillations to produce totally unsynchronized, individually chaotic behavior, or we can produce strongly synchronized chaotic oscillations of both the bursts and the faster spikes. Furthermore by changing the polarity of the coupling, we can set the system in a state of regular, out-of-phase oscillations.

These various states represent a sequence of bifurcations in the behavior of the coupled PD neurons as we vary the strength and polarity of the electrical coupling between them. When the total coupling (which we have called g_{ec} in this paper to compare with the results of the model) is made positive and large, the oscillations of both bursts and spikes are synchronized. As g_{ec} nears zero, the neurons decouple and show membrane voltage activity that is independent and chaotic. As g_{ec} is made negative, the neurons individually regularize their oscillations and perform out-of-phase spiking-bursting activity.

Using a model developed to describe the chaotic behavior of individual neurons in the lobster STG, we have shown that the connection of model PD neurons with electrical coupling between the soma regions of each neuron leads to behavior that is in striking correspondence with the experimental observations. This correspondence provides significant support for the model itself, and also shows that the origin of the observed chaotic behavior of the individual neurons is dynamic and not due to environmental noise.

The model of two electrically coupled PD neurons presented here incorporates enough biologically realistic ionic currents and enough detailed description of the calcium dynamics inside the cells that it allows a very direct comparison with experimental results. The success in characterizing the experimentally observed regimes of synchronization, nonsynchronization, and out-of-phase regularized synchronization supports its use to test hypotheses related to the role played by intracellular processes in the origin and control of irregular behavior observed in real neurons and neural circuits (Abarbanel et al. 1996).

An essential question raised by the observation of chaos in the individual neurons of CPGs is how an assembly of such neurons can cooperatively act to produce regular ordered signals that are useful in directing motor systems. In this paper we have explained how the slow calcium oscillations inside the ER may regulate chaotic bursting activity between two electrically coupled neurons. In the model, as long as the luminal calcium concentration remains essentially constant, the neuronal oscillations will be regular. This is a prediction that can be tested experimentally and is supported by recent studies showing that the presence of calcium oscillations inside the ER has important effects on the cytoplasmic membrane potential oscillations (Li et al. 1995a,b, 1997; Berridge 1998).

Our model makes an assumption about the role of calcium exchange between the intracellular medium and the ER, and this has yet to be verified experimentally. In this model the IP_3 concentration is the primary control parameter determining the appearance of chaos in the membrane voltage activity of single neurons. Whether this second messenger and its receptor are present in these CPG neurons is not yet experimentally established. However, there are several reports on the presence of IP_3 receptors in the ER of many excitable cells and neurons (Henzi and MacDermott 1992; Sharp et al. 1993; Berridge 1998). This leads us to expect that this receptor will be found in pyloric CPG neurons and that it acts to determine critical aspects of the calcium storage and release from the ER. From a strictly modeling point of view, any other mechanism as slow as calcium release and storage from the ER could act to initiate chaos in the membrane voltage time course and be responsible for its control induced by cooperative activity. From a biological point of view, the mechanism we utilize appears quite plausible.

In this paper we have focused on the use of a calcium dynamics and conductance based model and on the description of its behavior related to the synchronization and regularization of two electrically coupled neurons. We have also performed experiments and modeled single STG cells under periodic driving and two STG neurons connected with mutual inhibitory chemical synapses as we will describe elsewhere (Varona et al., in preparation). In these cases as well, the quantitative description of the observations by the models further suggest calcium concentration dynamics inside the ER as the main variable for the regularization process.

Finally, the success of this kind of model in both describing the chaotic oscillations of individual neurons in the pyloric CPG and characterizing quantitatively the synchronous and nonsynchronous behavior of two electrically coupled CPG neurons suggests that it would be worthwhile to look for the indicated calcium activity experimentally and provides clear support for the dynamic origin of chaotic activity in individual neural oscillations. Starting from this quantitative description of individual CPG neurons and the success, as reported here, of modeling synchronized, nonsynchronized, and regularized oscillations of two electrically coupled PD neurons, we are currently working on a description of more complex configurations in the CPG.

While of lesser biological importance, we wish to note that the results reported here have an impact on the study of synchronization of chaotic oscillators, which is quite important in the analysis of nonlinear dynamical systems (Abarbanel 1996). Essentially all of the work reported in the nonlinear dynamics literature is concerned with synchronization of physical systems connected either by diffusive couplings or via resistive couplings such as we have here. The oscillators discussed in the context of nonlinear dynamics have typically been invented or developed as simple examples for illustration of some point or another. To our knowledge, the dis-

cussion here and in Elson et al. (1998) represent the first times that a living system has been both observed and modeled as it undergoes a sequence of synchronized and unsynchronized coupled chaotic oscillations. This may give this example a rather broader interest than just within its biological setting.

Acknowledgements. We are most appreciative to A. I. Selverston, N. F. Rulkov, R. Huerta, and A. Szücs for many discussions on the model and on the experimental work reported in Elson et al. (1998). Partial support for this work came from NSF grants NCR-9612250 and IBN-96334405. P. Varona and J. J. Torres acknowledge support from MEC and Universidad de Granada, respectively. Mikhail Rabinovich acknowledges support from U.S. Department of Energy grant DE-FG03-96ER14592. Henry Abarbanel is supported in part by U.S. Department of Energy grant DE-FG03-90ER14138 and in part by NSF grant NCR-9612250. All authors received partial support from the CIA Office of Research and Development through project no. 98-F135000-000.

References

Abarbanel HDI (1996) Analysis of observed chaotic data. Springer, Berlin Heidelberg New York

Abarbanel HDI, Huerta R, Rabinovich MI, Rulkov NF, Rowat P, Selverston AI (1996) Synchronized action of synaptically coupled chaotic model neurons. Neural Comput 8: 1567–1602

Berridge MJ (1998) Neuronal calcium signaling. Neuron 21: 13–26

Elson R, Selverston AI, Huerta R, Rabinovich MI, Abarbanel HDI (1998) Synchronous behavior of two coupled biological neurons. Phys Rev Lett 81: 5692–5695

Falcke M, Huerta R, Rabinovich MI, Abarbanel HDI, Elson R, Selverston A (2000) Modeling observed chaotic oscillations in bursting neurons: the role of calcium dynamics and IP_3. Biol Cybern 82: 517–527

Henzi V, MacDermott AB (1992) Characteristics and function of Ca(2+)- and inositol 1,4,5-trisphosphate-releasable stores of Ca2+ in neurons. Neurosci 46: 251–273

Li Y-X, Keizer J, Stojilkovic SS, Rinzel J (1995) Ca^{2+} excitability of the ER membrane: an explanation for IP3-induced Ca^{2}_{+} oscillations. Am J Physiol 269: C1079–C1092

Li Y-X, Rinzel J, Stojilkovic SS (1995) Spontaneous electrical and calcium oscillations in unstimulated pituitary gonadotrophs. Biophys J 69: 785–795

Li Y-X, Stojilkovic SS, Keizer J, Rinzel J (1997) Sensing and refilling calcium stores in a excitable cell. Biophys J 72: 1080–1091

Martone ME, Alba SA, Edelman VM, Airey JA, Ellisman MH (1997) Distribution of inositol-1,4,5-trisphosphate and ryanodine receptors in rat neostriatum. Brain Res 293: 35–47

Otsu H, Yamamoto A, Maeda N, Mikoshiba K, Tashiro Y (1990) Immunogold localization of inositol 1,4,5-trisphosphate ($InsP_3$) receptor in mouse cerebellar Purkinje cells using three monoclonal antibodies. Cell Struct Funct 15: 163–173

Satoh T, Ross CA, Villa A, Supattapone S, Pozzan T, Snyder SH, Meldolesi J (1990) The inositol 1,4,5-trisphosphate receptor in cerebellar Purkinje cells: quantitative immunogold labeling reveals concentration in an ER Subcompartment. J Cell Biol 111: 615–625

Sharp AH, McPherson PS, Dawson TM, Aoki C, Campbell KP, Snyder SH (1993) Differential immunohistochemical localization of inositol 1,4,5-trisphosphate- and ryanodine-sensitive Ca2+ release channels in rat brain. J Neurosci 13: 3051–3063

Sharp AA, Abbott LF, Marder E (1992) Artificial electrical synapses in oscillatory networks. J Neurophysiol 67: 1691–1694

Walton PD, Airey JA, Sutko JL, Beck CF, Mignery GA, Südhof TC, Deerinck TJ, Ellisman MH (1991) Ryanodine and inositol trisphosphate receptors coexist in avian cerebellar Purkinje neurons. J Cell Biol 113: 1145–1157